PAPER

A novel label-free terbium(III)-aptamer based aptasensor for ultrasensitive and highly specific detection of acute lymphoma leukemia cells

Siwen Wu, [ID] † Nuo Yang,† Liping Zhong, Yiqun Luo, Huiling Wang, Wenlin Gong, Sufang Zhou, Yanmei Li, Jian He, Haopei Cao, Yong Huang* and Yongxiang Zhao*

Acute leukemia is a malignant clonal disease of hematopoietic stem cells with a high prevalence and mortality rate. However, there are no efficient tools to facilitate early diagnosis and treatment of leukemia. Therefore, development of new methods for the early diagnosis and prevention of leukemia, especially non-invasive diagnosis at the cellular level, is imperative. Here, a label-free signal-on fluorescence aptasensor based on terbium(III)-aptamer (Tb^{3+}-apt) was applied for the detection of leukemia. The aptamer sensitizes the fluorescence of Tb^{3+} and forms the strong fluorescent Tb^{3+}-apt probe. The target cells, the T-cell acute lymphoblastic leukemia cell line (CCRF-CEM) combined with the Tb^{3+}-apt probe to form the Tb^{3+}-apt–CEM complex, were removed by centrifugation, and the supernatant containing a small amount of the Tb^{3+}-apt probe was detected using a fluorescence spectrophotometer. The logarithm of cell concentration showed a good linear relationship ($R^2 = 0.9881$) with the fluorescence signal. The linear range for CCRF-CEM detection was $5-5 \times 10^6$ cells per ml, while the detection limit was 5 cells per ml of the binding buffer. Clinical samples were collected from 100 cases, and the specificity and positive rates detected by this method were up to 94% and 90%, respectively. Therefore, a single-stranded DNA-sensitized terbium(III) luminescence method diagnostic was developed which is rapid, sensitive, and economical and can be used for diagnosis of various types of leukemia at the early stage.

1. Introduction

Presently, the threat to human health and life due to high incidence and mortality of refractory cancers is rising annually.[1] Acute lymphoblastic leukemia is a common and fatal cancer that usually begins in the bone marrow, and is characterized by the presence of a large number of immature white blood cells in children and adolescents.[2,3] This disease not only demands a lot of medical and health resources, but also negatively affects the people's living standards and social welfare. Acute leukemia can lead to abnormal proliferation and accumulation of primary cells in the bone marrow and inhibit hematopoietic development, leading to anemia, thrombocytopenia and neutropenia. Moreover, the primary cells can also infiltrate the liver, spleen and other external tissues to cause corresponding lesions.[2] Extracting peripheral blood cells and

the bone marrow is one of the mainstay methods used to detect leukemia in clinics, although other testing methods are used,[3] including fluorescent labeling,[4–6] cytochemistry,[7,8] flow cytometry,[9–11] immunohistochemical[12,13] and immunophenotype analysis, and aptamer-conjugated polymeric nanoparticles.[14,15] However, most of these methods not only are costly, time-consuming, complicated and labor-intensive, but also require a combination of sophisticated instruments, which have low sensitivity and demand multiple step processing making them unsuitable for simple and rapid medical analysis. Therefore, there is a need to explore a highly specific, sensitive and cost-effective method to facilitate early diagnosis and treatment of leukemia. This especially demands for non-invasive diagnostic and prevention techniques targeted at the cellular level based on modern analytical chemistry to improve the treatment and survival rates of the patients.

In order to get highly specific targeting probes, scientists have used systematic evolution of ligands by exponential enrichment (SELEX) to screen for the new type of molecular recognition elements – nucleic acid aptamers.[16–18] Due to their characteristic high affinity to target molecules, aptamers are often referred to as "chemical antibodies".[19] Compared with antibodies, aptamers are cheaper, less invasive and easily

National Center for International Research of Bio-targeting Theranostics, Guangxi Key Laboratory of Bio-targeting Theranostics, Collaborative Innovation Center for Targeting Tumor Diagnosis and Therapy, Guangxi Medical University, Nanning, Guangxi 530021, China. E-mail: yongxiang_Zhao@126.com, huangyong503@126.com; Fax: (+86) 771-5317 061; Tel: (+86) 771-5317 061
†These authors contributed equally to this work.

reproducible due to the unambiguous primary structure.[20–22] Aptamers can bind not only to inorganic ions, small molecules, biological macromolecules, but also to supramolecular substances such as cells, viruses, and pathological tissue sections.[23–25] Moreover, the synthesis of aptamers is easy and uses short cycles,[26,27] and aptamers show good stability[28] and are easy to modify.[29,30] The emergence of aptamers has provided a new identification tool to the biochemistry and the biomedical communities. In recent years, nucleic aptamer-based biosensors have shown promising applications in the detection of cancer.[31,32] In 2006, Tan *et al.* first selected the live tumor cell line,[33] human acute lymphoblastic leukemia cell line CCRF-CEM, as target cells to screen for high specificity and affinity sgc8 aptamers. Subsequently, the sgc8 aptamer has found wide usage in the detection of acute lymphoblastic leukemia.[34,35]

Rare earth terbium ion (Tb^{3+}) is a promising non-labeled fluorescent probe that has attracted a great deal of attention[36] because of its unique optical properties, such as a long fluorescence lifetime, large Stokes shift and narrow emission band.[37,38] Fu *et al.* reported that single-stranded oligonucleotides can enhance the fluorescence of rare earth terbium ions (Tb^{3+}), but not the double-stranded DNA.[39] Another study reported that G base-rich single-stranded oligonucleotides can effectively sensitize the fluorescence of Tb^{3+}.[40] Based on these reports, Wei *et al.* designed a G-base-rich hairpin probe which sensitizes the Tb^{3+} fluorescence. The heavy metal lead (Pb^{2+}) competitively binds this hairpin probe to quench the fluorescence of Tb^{3+}. This strategy allows a highly sensitive non-labeled detection of Pb^{2+} (detection limit of 0.1 nM).[41]

Inspired by the above studies, this study leveraged on the characteristics of nucleic acid aptamers and single-stranded DNA sensitized rare earth Tb^{3+} fluorescence to design a non-labeled signal-sensitive fluorescence method for the detection of CCRF-CEM cells. This method is based on the principle that the aptamer sensitizes the fluorescence of Tb^{3+} and forms a strong fluorescent Tb^{3+}-apt probe. After the target cells CCRF-CEM combined with Tb^{3+}-apt to form a Tb^{3+}-apt–CEM complex, the supernatant is obtained by centrifugation, and then the supernatant was detected by fluorescence spectrophotometer. The concentration of CCRF-CEM cells in $5–5 \times 10^6$ cells per ml showed a good linear relationship between the logarithmic value and the fluorescence signal ($R^2 = 0.9881$), and the detection limit was up to 5 cells per ml. This label-free signal sensitized fluorescence method has the advantages of high selectivity, easy operation and rapidity and is expected to provide a robust, simple, and inexpensive novel method for the ultrasensitive diagnosis of acute lymphoblastic leukemia.

2. Experimental

2.1. Materials

The label-Free Sgc8 aptamer (apt) with a sequence of 5′-ATCTAACTGCTGC GCCGCCGGGAAAATACTGTACGGTTAGA-3′ and the label-Free random aptamer (apt-) with a sequence of

5′-ATGTGGCTGCTGCGCCGCCGGGA AAATACTGT ACGGTTAGA-3′ were purchased from Shanghai Sangon Biological Engineering Technology & services (Shanghai, China). 4-(2-hydroxyethyl) piperazine-1-ethanesulfonic acid (HEPES, pH = 7.2–7.4, >99.5%) and the nitrate of metal salts (>99%), including potassium (K^+), sodium (Na^+), silver (Ag^+), magnesium (Mg^{2+}), calcium (Ca^{2+}), copper (Cu^{2+}), zinc (Zn^{2+}), iron (Fe^{3+}), and terbium (Tb^{3+}), were purchased from Sigma-Aldrich, Inc. All solutions were produced with ultra-pure water of 18.2 MΩ purified from a Milli-Q purification system (Milli-Pore, Bedford, MA, USA). CCRF-CEM, Ramos (human Burkitt's lymphoma cell lines) cells, and K562 (chronic myelocytic leukemia cell lines), HL-60 (human promyelocytic leukemic cell lines), Thp-1 (mononuclear phagocyte system) and U937 (tissue cell lymphoma cells) cell lines were purchased from the Cell Bank of the Chinese Academy of Sciences (Shanghai, China).

2.2. Instruments

All fluorescence measurements were carried out in a 350 μL quartz cuvette. The excitation wavelength was 292 nm, and the emission spectra were recorded with both excitation and emission slits of 5 nm using an F-7000 fluorescence spectrophotometer (Hitachi Company, Tokyo, Japan). The peak intensities were obtained at 545 nm, and the sampling range was recorded from 460 nm to 560 nm. All the atomic force microscopy imaging was performed by fluorescence microscopy (Nikon DS-Ri1; Nikon, Tokyo, Japan). Cell Counting Kit-8 was bought from Dojindo, Japan.

2.3. Cell culture

CCRF-CEM, Ramos cells, and K562, HL-60, Thp-1 and U937 cell lines were cultured in 5% carbon dioxide (95% oxygen) at 37 °C for 3 days and the medium of 1640 which contained 10% fetal bovine serum (FBS, Gibco) and 100 U mL^{-1} penicillin–streptomycin (Gibco, Grand Island, NY, USA).

2.4. Preparation of the Tb^{3+}-apt fluorescent aptasensor

A suitable aptamer (50 μM) diluted by 252 μl PBS (phosphate-buffered saline, 10 mM, pH 7.2) and Tb^{3+} solution diluted by the same volume HEPES buffer (200 mM, 1 mM magnesium nitrate, pH 7.2) were put in storage solution at 4 °C in the dark. Magnesium ions were used to stabilize the oligonucleotides' conformation and decrease the non-specific binding between other metal ions and the oligonucleotides. The final concentrations of the oligonucleotides (5 μM oligonucleobases) and terbium nitrate (20 mM) were prepared in PBS. For example, an application-type mixture (5 μM oligonucleobases, 20 mM Tb^{3+}) was formed by adding 160 μl PBS to 40 μl storage solution.

2.5. Optimization of the fluorescent aptasensor

To optimize the Tb^{3+} concentration and detection conditions, the probe preparation method is the same as the preparation of the Tb^{3+}-apt fluorescent aptasensor above, just fixing one condition to optimize the others. Different concentrations of

Tb^{3+} (5 mM, 10 mM, 15 mM, 20 mM, 25 mM, 30 mM) with oligonucleotides (5 μM) were detected. In order to explore the effect of pH value on fluorescence intensity of Tb^{3+}, the fluorescence intensity of Tb^{3+} (20 mM) with oligonucleotides (5 μM) in the application-type mixture (pH 4.8, pH 6.0, pH 7.2, pH 8.4, pH 9.6, pH 11.0, pH 12.0, pH 13.0) was detected. And the fluorescence intensity of Tb^{3+} (20 mM) with oligonucleotides (5 μM) after incubation with CCRF-CEM (1×10^6 cells per 200 μl) at room temperature for different time periods (5 min, 10 min, 20 min, 30 min, 40 min, 60 min) was also detected. All cell samples were centrifuged at 1000 rpm for 3 min, then 160 μl of the supernatant was collected, and the pH value was adjusted to 9.6 for detection by fluorescence spectroscopy at the wavelength range of 460 nm–560 nm. Fluorescence intensity of Tb^{3+} (20 mM) with oligonucleotides (5 μM) after 10 min of incubation with CCRF-CEM (1×10^6 cells per 200 μl) at 4 °C, 25 °C and 37 °C was detected, too. Data are expressed as the mean ± SD of 3 independent experiments; the difference between fluorescence intensities obtained by the rank sum test is statistically significant ($P < 0.05$).

2.6. Probe for the detection of cells

A suitable aptamer (50 μM) diluted by 252 μl PBS (10 mM, pH 7.2) and a Tb^{3+} solution diluted by the same volume of HEPES buffer (200 mM, 1 mM magnesium nitrate, pH 7.2) were used to prepare the probe storage solution at 4 °C in the dark. 1 ml of CCRF-CEM cells were collected after centrifugation, the cells were washed three times with PBS, and then the supernatant was drained and re-suspended in 160 μl PBS. Finally, 40 μl of probe storage solution was added and mixed well. The different concentrations of CCRF-CEM cells (1 to 1×10^6 cells per 200 μl) were incubated with the Tb^{3+}-apt fluorescent aptasensor at 4 °C in the dark for 10 min. The samples were centrifuged at 1000 rpm for 3 min, then 160 μl of the supernatant was collected, and the pH value was adjusted to 9.6 for detection by fluorescence spectroscopy at the wavelength range of 460 nm–560 nm.

2.7. Specificity assay

The fluorescence spectrophotometer detected different blood-related cancer cells. To investigate the specificity of the Tb^{3+}-apt fluorescent aptasensor, an F-7000 fluorescence spectrophotometer and a confocal fluorescence microscope were used to test different cells, including CCRF-CEM, HL-60 cells, Ramos cells, K562 cells, PBL cells (peripheral blood lymphocytes), Thp-1 cells and U937 cells. Each of the 200 μl reaction systems including 1×10^6 cells was centrifuged at 1000 rpm for 3 min to collect 160 μl (removing fluid that may contain cells at the bottom of 40 μl) of the supernatant, and the pH value was adjusted to 9.6 for detection using the F-7000 fluorescence spectrophotometer.

Immunofluorescence imaging was performed in different blood-related cancer cells. Cells were collected in a 1.5 ml centrifugation tube, washed three times with PBS, incubated with the Tb^{3+}-apt fluorescent aptasensor at 4 °C in the dark for 10 min and then washed again with PBS. The cells were fixed with 4% paraformaldehyde (Sigma-Aldrich, St Louis, MO, USA) for 10 min, washed with PBS, and stained with 4′,6-diamidino-2-phenylindole dihydrochloride (DAPI; Life Technologies, Foster City, CA, USA) for 5 min in the dark. The cells were finally washed with PBS and examined by fluorescence microscopy.

2.8. Detection of clinical samples

Blood samples were collected from 20 ALL (acute lymphoblastic leukemia) patients, 60 non-ALL patients, and 20 normal subjects based on clinically diagnosed classifications. All samples were from the First Affiliated Hospital of Guangxi Medical University. These experiments were approved by the Ethics Committee of Guangxi Medical University, and patient's informed consent was obtained before the experiment. 5 ml of peripheral blood of each case was obtained with anticoagulants, and human peripheral blood lymphocyte separation solution (Solarbio, Cat. No. P8610) was added for gradient centrifugation at a rotation speed of 1000g for 30 min. The white film layer between plasma and separation solution was taken. 200 μl of the reaction systems (detection of the cell reaction system above) was added, incubated for 10 min, and then centrifuged at 1000 rpm for 3 min. 160 μl of the supernatant was obtained, the pH value was adjusted to 9.6, and the supernatant fluorescence was detected using the F-7000 fluorescence spectrophotometer.
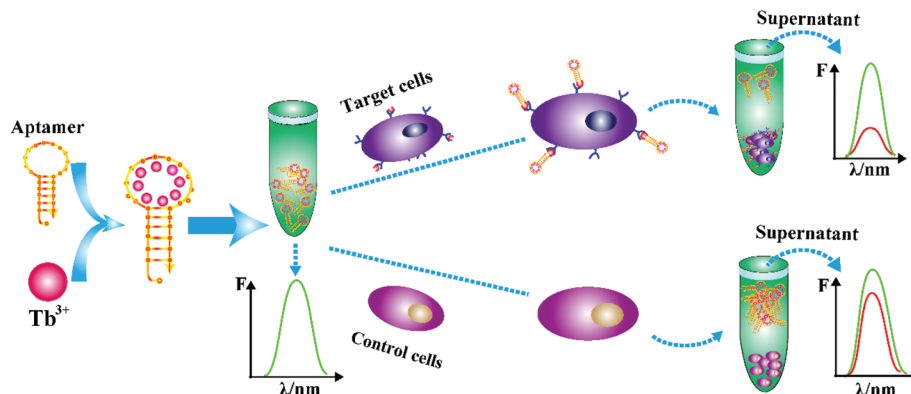
2.9. Statistical analyses

Each experiment was carried out in triplicate. Data are expressed as the mean ± SD or as the median (range). All statistical analyses were performed using GraphPad Prism 6.02 (GraphPad Software, San Diego, CA, USA). $P < 0.05$ was considered statistically significant.

3. Results and discussion

3.1. Principle of the Tb^{3+}-apt fluorescent aptasensor

Based on the characteristics of nucleic acid aptamers and single-stranded DNA sensitized rare earth Tb^{3+} fluorescence, a label-free signal sensitized fluorescence method was developed in this study for the detection of CCRF-CEM cells in acute lymphoblastic leukemia. The detection principle is shown in Scheme 1. The hairpin type single-chain aptamer (the yellow hairpin structure sequence in the figure) can sensitize Tb^{3+} (green particles in the figure) fluorescence. The Tb^{3+}-apt probe can recognize the CCRF-CEM cells specifically to form the Tb^{3+}-apt–CEM complex, and the supernatant of the Tb^{3+}-apt–CEM complex collected by centrifugation may be used for fluorescence detection. Compared with the Tb^{3+}-apt–nontarget cells complex, the fluorescence signal of the corresponding supernatant was significantly reduced. In contrast, in the absence of the CCRF-CEM cells, the Tb^{3+}-apt probe was still present in the supernatant and there was no significant change in the fluorescence strength.

Scheme 1 Schematic illustration of the Tb^{3+}-apt fluorescent aptasensor for detection of CCRF-CEM cells.

3.2. Characterization of Tb^{3+} fluorescence

The feasibility of this method was first verified by fluorescence spectroscopy, and the results are shown in Fig. 1A. The fluorescence intensity of Tb^{3+}-apt was the strongest. When the non-target Romas cells were added to the Tb^{3+}-apt probe solution, there was barely any change in the fluorescence intensity, whereas the fluorescence intensity was significantly decreased

when the CEM cells were added. And when the non-target G-base rich single stranded oligonucleotides Tb^{3+}-apt(−) were incubated with the CEM cells, the fluorescence intensity was hardly attenuated. A statistical graph showed similar results (Fig. 1B). The PTK7 protein on the surface of the CEM cell membrane specifically binds to the Sgc8 aptamer, and the target cells then removed the probe by centrifugation, leaving almost no Tb^{3+}-apt probe in the supernatant, leading to a
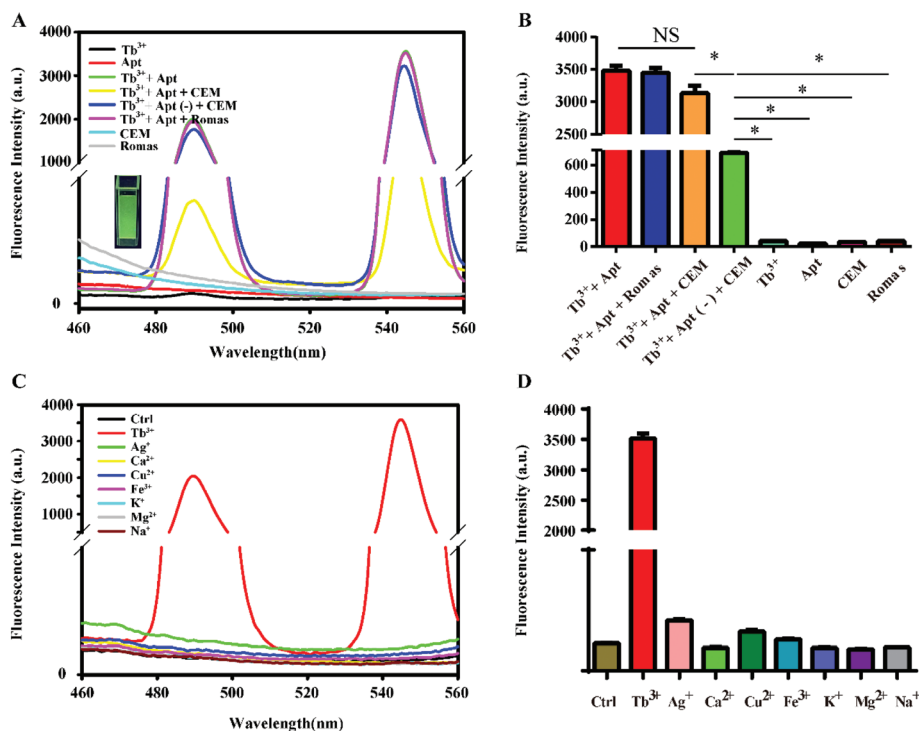

Fig. 1 (A) Fluorescence emission spectra of Tb^{3+}, apt and CCRF-CEM cells under different conditions: Tb^{3+}; Apt (5 uM); Tb^{3+} + apt; Tb^{3+} + apt + CCFF-CEM; Tb^{3+} + apt(−) + CCFF-CEM; Tb^{3+} + apt + Romas; Tb^{3+} (20 mM); CCRF-CEM (1 × 10⁶ cells); Romas (1 × 10⁶ cells). Excitation: 290 nm. (B) Quantitative analysis of fluorescence emission spectra of Tb^{3+}, apt, apt(−) and CCRF-CEM under different conditions. NS, not statistically significant, *P < 0.05, statistically significant. (C) Fluorescence emission spectra of the aptamer with different metal ions. When the Sgc8 aptamer combines with the terbium ion, the fluorescence is markedly enhanced, whereas the other metal ions barely show any fluorescence when mixed with the Sgc8 aptamer. (D) Statistical analysis of fluorescence emission spectra of the aptamer with different metal ions, showing significant differences between Tb^{3+} and other ions that mixed with the aptamer.

rapid decrease of the fluorescence. While the individual Tb^{3+}, apt, CEM, and Romas cells are almost non-fluorescent, the Tb^{3+}-apt probe emits green fluorescence under ultraviolet light. In order to confirm the characteristics of Tb^{3+} sensitized specificity of DNA, Tb^{3+} and other different ions in the physical environment were reacted with aptamers. The results showed that when the aptamer binds to the terbium ion, the fluorescence is markedly enhanced, whereas the other metal ions (including K^+, Na^+, Ag^+, Cu^{2+}, Zn^{2+}, Mg^{2+}, Ca^{2+}, Fe^{3+}) show almost no fluorescence when they are bound to the aptamer (Fig. 1C), and a statistical graph of the reaction of Tb^{3+} and other different ions with aptamers showed a similar trend (Fig. 1D). This result also indicates that the hairpin type single-chain aptamer can sensitize Tb^{3+} fluorescence. However, silver, calcium, copper, iron, potassium, magnesium, and sodium ions do not have this function. The specific principle is similar to the hairpin structure of aptamers that may be affected by the coordination of strontium ions and aptamer polyguanine rings studied.[41]

3.3. Experimental condition optimization

The experimental conditions were optimized, and the results are shown in Fig. 2. The aptamer concentration was fixed at 5 μM, and the Tb^{3+} concentration was then optimized. When the concentration of Tb^{3+} was 20 mM, the fluorescence intensity was the highest (Fig. 2A), so 20 mM Tb^{3+} was selected as

the optimal concentration. By adjusting the pH of the probe (Tb^{3+}-apt) solution, it was found that the fluorescence was strongest when the pH was 9.6; thus, pH = 9.6 was chosen (Fig. 2B). When the incubation time was in the range of 5 to 10 min, the fluorescence intensity increased with time, while the incubation time in the range of 10 to 30 min led to a plateau in the fluorescence intensity. Considering the time efficiency, 10 min was selected as the optimum incubation time for follow-up experiments (Fig. 2C). At the same time, the fluorescence was most intense when incubated at 4 °C (Fig. 2D); therefore, 4 °C was chosen as the optimal hybridization temperature.

3.4. Analytical performance of the aptasensor

Under the selected optimal conditions, the sensitivity of the fluorescence method was examined. As shown in Fig. 3A, the difference in the fluorescence intensity gradually decreases with the increase of the concentration of the CEM cells (a. Tb^{3+}-apt; b. 10^0 cells per 200 μl, c. 10^1 cells per 200 μl, d. 10^2 cells per 200 μl, e. 10^3 cells per 200 μl, f. 10^4 cells per 200 μl, g. 10^5 cells per 200 μl, h. 10^6 cells per 200 μl). In the range of 1 to 10^6 cells per 200 μl, the logarithm of the concentration of the CEM cells showed a good linear relationship with the fluorescence signal, the fluorescence intensity as a function of Tb^{3+}-apt minus logarithm of concentration of the cells. The results were the average of four repetitive experiments, with
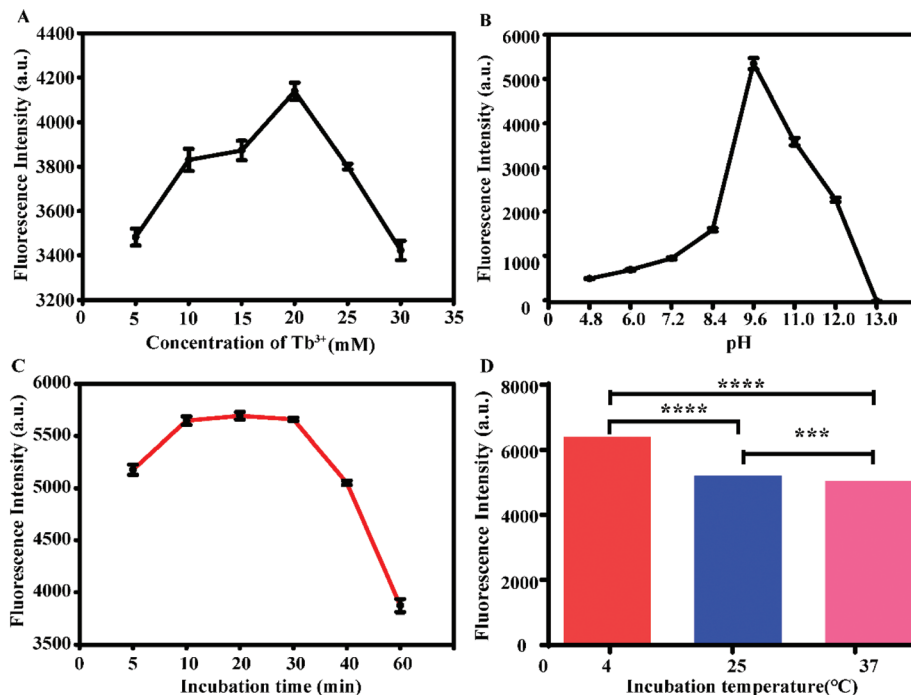

Fig. 2 Optimization of Tb^{3+} concentration and detection conditions. (A) Concentration of Tb^{3+} (5 mM, 10 mM, 15 mM, 20 mM, 25 mM, 30 mM) with oligonucleotides (5 μM). (B) Fluorescence intensity of Tb^{3+} (20 mM) with oligonucleotides (5 μM) in the application-type mixture (pH 4.8, pH 6.0, pH 7.2, pH 8.4, pH 9.6, pH 11.0, pH 12.0, pH 13.0). (C) Fluorescence intensity of Tb^{3+} (20 mM) with oligonucleotides (5 μM) after incubation with CCRF-CEM (1×10^6 cells per 200 μl) at room temperature for different incubation periods. (D) Fluorescence intensity of Tb^{3+} with oligonucleotides in the application-type mixture (5 μM oligonucleobases, 20 mM Tb^{3+}, pH 7.2) after 10 min of incubation with CCRF-CEM (1×10^6 cells per 200 μl) at 4 °C, 25 °C and 37 °C. Data are expressed as the mean ± SD of 3 independent experiments; ***$P < 0.001$.
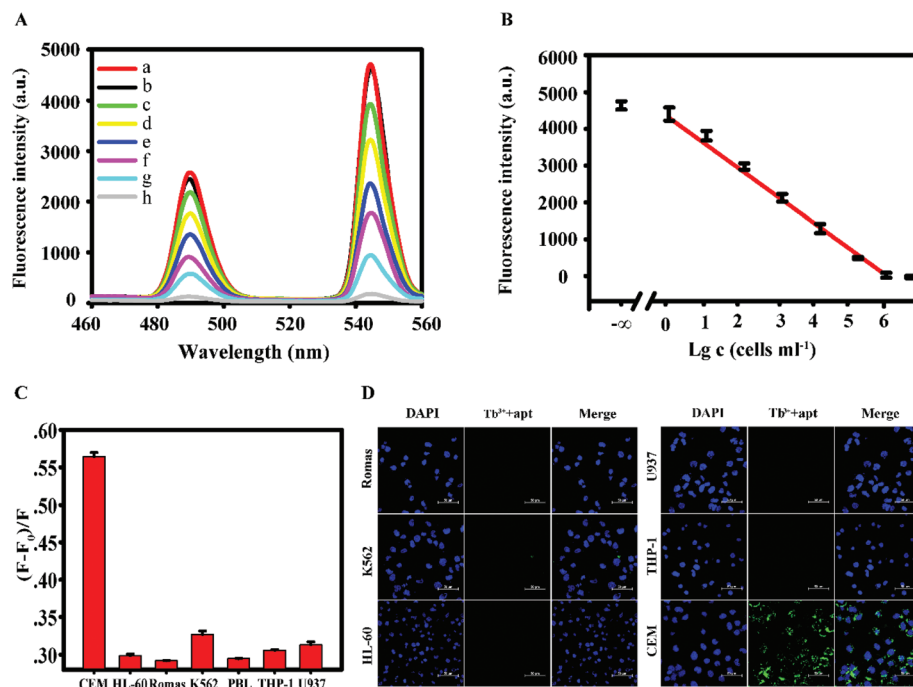
Fig. 3   (A) Fluorescence emission spectra of the Tb^{3+}-apt fluorescent aptasensor in the presence of different concentrations of CCRF-CEM cells (a. Tb^{3+}-apt, b. 10^0 cells per 200 μl, c. 10^1 cells per 200 μl, d. 10^2 cells per 200 μl, e. 10^3 cells per 200 μl, f. 10^4 cells per 200 μl, g. 10^5 cells per 200 μl, h. 10^6 cells per 200 μl). (B) Linear relationship between the fluorescence intensity and the concentration of CCRF-CEM cells. (C) Specificity of the fluorescent aptasensor for CEM. The fluorescence intensity rate $(F − F_0)/F$ of the Tb^{3+}-apt fluorescent aptasensor in the presence of CEM, HL-60, Ramos, K562, PBL, THP-1, and U937 cells, respectively (1×10^6 cells per 200 μl), where F and F_0 are the fluorescence intensity without and with detection cells at 545 nm. Excitation: 290 nm. (D) Fluorescence micrographs of six different cells after mixing with Tb^{3+}-apt. Nuclei were stained with DAPI. Scale bars indicate 50 μm.

Table 1   Comparison of analytical properties of CCRF-CEM cytosensors

Detection method	Linear range	Detection limit/mL	Ref.
Colorimetric	3.30×10^3–2.69×10^3	214	42
Quartz crystal microbalance	8.00×10^3–1.00×10^5	8000	43
Aptamer-conjugated magnetic beads	1.00×10^4–1.50×10^5	8000	44
Flow cytometry	7.50×10^3–6.25×10^5	750	45
Fluorescence	5.00–5.00×10^6	5	This work

error bars indicating the standard deviation (Fig. 3B). The linear equation was $F = −680.2C + 5750.6$ (F is the fluorescence intensity, C is Tb^{3+}-apt minus logarithm of concentration of the cells), $R^2 = 0.9881$, and the detection limit is 5 cells per ml. Compared with other reported fluorescence methods in Table 1, this method can significantly reduce the detection limit, suggesting a better sensitivity.

Under the selected optimal conditions, the specificity of the fluorescence method was investigated. According to the results shown in Fig. 3C, the intensity of fluorescence of the CEM cells was significantly higher than that of other control cells. In addition, as shown in Fig. 3D, the probes bound well to the target cell CEM as detected using the confocal microscope, emitting green fluorescence, whereas the probes did not bind to other cells, as only blue nuclei could be seen. These experi-
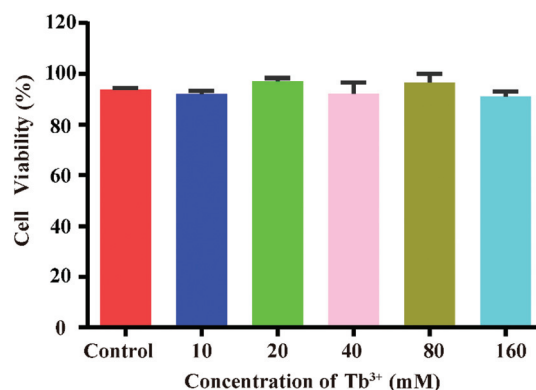

Fig. 4   Relative viability of CCRF-CEM cells incubated with Tb^{3+}-apt at different concentrations for 24 h.

Table 2 General clinical information

Number	Gender	Age (years)	Sample	Diagnosis
			Acute lymphoblastic leukemia patients (ALL)	
1	Female	28	Peripheral blood/bone marrow	T-ALL-L1
2	Female	13	Peripheral blood	T-ALL-L2
3	Male	6	Peripheral blood/bone marrow	T-ALL-L1
4	Male	8	Peripheral blood/bone marrow	T-ALL-L1
5	Female	9	Peripheral blood/bone marrow	T-ALL-L2
6	Male	20	Peripheral blood/bone marrow	T-ALL-L2
7	Male	12	Peripheral blood/bone marrow	T-ALL-L1
8	Male	19	Peripheral blood/bone marrow	T-ALL-L1
9	Male	29	Peripheral blood/bone marrow	T-ALL-L2
10	Female	5	Peripheral blood/bone marrow	T-ALL-L1
11	Female	34	Peripheral blood/bone marrow	T-ALL-L1
12	Male	8	Peripheral blood/bone marrow	T-ALL-L2
13	Male	9	Peripheral blood/bone marrow	T-ALL-L1
14	Female	15	Peripheral blood/bone marrow	B-ALL
15	Female	12	Peripheral blood/bone marrow	T-ALL-L1
16	Male	54	Peripheral blood/bone marrow	T-ALL-L2
17	Male	2	Peripheral blood/bone marrow	T-ALL-L2
18	Male	9	Peripheral blood/bone marrow	T-ALL-L1
19	Male	6	Peripheral blood/bone marrow	T-ALL-L1
20	Female	6	Peripheral blood/bone marrow	T-ALL-L2
			Acute myelocytic leukemia patients (AML)	
1	Male	59	Peripheral blood/bone marrow	AML-M1
2	Male	33	Peripheral blood/bone marrow	AML-M3
3	Female	65	Peripheral blood/bone marrow	AML-M0
4	Male	45	Peripheral blood/bone marrow	AML-M1
5	Female	58	Peripheral blood/bone marrow	AML-M1
6	Male	13	Peripheral blood/bone marrow	AML-M1
7	Male	10	Peripheral blood/bone marrow	AML-M1
8	Female	5	Peripheral blood/bone marrow	AML-M1
9	Female	5	Peripheral blood/bone marrow	AML-M3
10	Male	8	Peripheral blood/bone marrow	AML-M4
11	Male	54	Bone marrow	AML-M3
12	Male	7	Peripheral blood/bone marrow	AML-M3
13	Female	31	Bone marrow	AML-M3
14	Male	21	Peripheral blood/bone marrow	AML-M3
15	Female	54	Peripheral blood/bone marrow	AML-M1
16	Male	23	Peripheral blood/bone marrow	AML-M1
17	Female	5	Peripheral blood/bone marrow	AML-M1
18	Female	18	Bone marrow	AML-M3
19	Male	17	Peripheral blood/bone marrow	AML-M1
20	Male	17	Peripheral blood/bone marrow	AML-M4
			Chronic lymphocytic leukemia (CLL)	
1	Male	58	Peripheral blood/bone marrow	B-CLL
2	Male	45	Peripheral blood/bone marrow	B-CLL
3	Male	57	Peripheral blood/bone marrow	B-CLL
4	Female	6	Peripheral blood/bone marrow	B-CLL
5	Female	8	Bone marrow	B-CLL
6	Female	9	Peripheral blood/bone marrow	B-CLL
7	Female	12	Bone marrow	B-CLL
8	Female	7	Peripheral blood	B-CLL
9	Male	5	Peripheral blood/bone marrow	B-CLL
10	Male	16	Peripheral blood/bone marrow	B-CLL
11	Male	23	Peripheral blood/bone marrow	T-CLL
12	Male	18	Bone marrow	B-CLL
13	Male	17	Peripheral blood/bone marrow	B-CLL
14	Female	25	Peripheral blood/bone marrow	B-CLL
15	Female	29	Peripheral blood/bone marrow	B-CLL
16	Female	5	Peripheral blood/bone marrow	T-CLL
17	Male	6	Peripheral blood	B-CLL
18	Male	6	Peripheral blood	B-CLL
19	Female	8	Bone marrow	B-CLL
20	Female	59	Peripheral blood/bone marrow	B-CLL
			Other	
1	Male	56	Peripheral blood/bone marrow	Myelodysplastic histiocytosis
2	Male	34	Peripheral blood/bone marrow	Myelodysplastic histiocytosis
3	Female	26	Peripheral blood/bone marrow	Myelodysplastic histiocytosis
4	Male	21	Peripheral blood/bone marrow	Myelodysplastic histiocytosis
5	Male	5	Peripheral blood/bone marrow	Thrombocytopenic purpura
6	Female	14	Peripheral blood/bone marrow	Thrombocytopenic purpura

Table 2 (Contd.)

Number	Gender	Age (years)	Sample	Diagnosis
7	Male	12	Peripheral blood/bone marrow	Non-Hodgkin's lymphoma
8	Male	52	Peripheral blood/bone marrow	Non-Hodgkin's lymphoma
9	Female	51	Peripheral blood/bone marrow	Thrombocytopenic purpura
10	Female	25	Peripheral blood/bone marrow	Iron deficiency anemia
11	Female	18	Peripheral blood/bone marrow	Iron deficiency anemia
12	Male	15	Peripheral blood/bone marrow	Iron deficiency anemia
13	Female	14	Peripheral blood/bone marrow	The Mediterranean anemia
14	Male	16	Peripheral blood/bone marrow	The Mediterranean anemia
15	Male	29	Peripheral blood/bone marrow	The Mediterranean anemia
16	Female	38	Peripheral blood/bone marrow	The Mediterranean anemia
17	Male	45	Peripheral blood/bone marrow	The Mediterranean anemia
18	Female	56	Peripheral blood/bone marrow	Hodgkin's lymphoma
19	Male	29	Peripheral blood/bone marrow	Hodgkin's lymphoma
20	Male	37	Peripheral blood/bone marrow	Hodgkin's lymphoma
			Healthy volunteers Normal	
1	Female	18	Peripheral blood	Normal
2	Male	20	Peripheral blood	Normal
3	Male	25	Peripheral blood	Normal
4	Female	24	Peripheral blood	Normal
5	Male	24	Peripheral blood	Normal
6	Male	48	Peripheral blood	Normal
7	Female	45	Peripheral blood	Normal
8	Male	34	Peripheral blood	Normal
9	Male	35	Peripheral blood	Normal
10	Male	28	Peripheral blood	Normal
11	Male	28	Peripheral blood	Normal
12	Male	27	Peripheral blood	Normal
13	Female	26	Peripheral blood	Normal
14	Male	26	Peripheral blood	Normal
15	Male	26	Peripheral blood	Normal
16	Male	27	Peripheral blood	Normal
17	Male	25	Peripheral blood	Normal
18	Male	25	Peripheral blood	Normal
19	Female	24	Peripheral blood	Normal
20	Male	24	Peripheral blood	Normal

Table 3 Comparison of clinical diagnosis rate and detection rate of this experimental method

Group	Number of clinical diagnoses	Number of diagnoses by this experimental method
ALL group	20	18
Non-ALL group and the normal group	80	5

ALL, acute lymphoblastic leukemia.

mental results show that this method has strong anti-interference and high specificity for CEM cells.

3.5. The cytotoxicity of the probe

In order to investigate whether the apt-Tb^{3+} probe is destructive to the sample during the assay, *in vitro* toxicity assessment was performed at the cellular level using the Cell Counting Kit-8. The CEM cells were co-cultured with different concentrations of probes, and the cell viability was measured after co-culture for a certain period. Fig. 4 shows that as the probe concentration increases (10 mM, 20 mM, 40 mM, 80 mM, 160 mM), the viability of the cells is reduced, but even at a

maximum concentration of 160 mM, the probe is incubated with the CEM cells for 4 h; therefore, the vitality can be preserved above 90%. This result indicates that the probe has
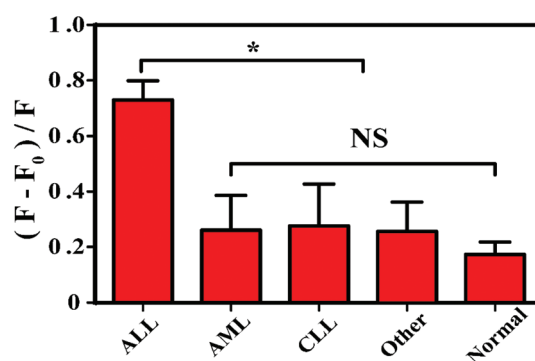

Fig. 5 Specificity of the fluorescent aptasensor for clinical samples. The fluorescence intensity rate $(F - F_0)/F$ of the Tb^{3+}-apt fluorescent aptasensor in the presence of ALL (acute lymphoblastic leukemia), AML (acute myelocytic leukemia), CLL (chronic lymphocytic leukemia), other (including myelodysplastic histiocytosis, Hodgkin's lymphoma, non-Hodgkin's lymphoma, thrombocytopenic purpura, iron deficiency anemia, the Mediterranean anemia), normal, where F and F_0 are the fluorescence intensity without and with detection cells at 545 nm. Excitation: 290 nm.

good biocompatibility with no toxicity to cells during a short period.

3.6. Analysis of clinical samples

In order to evaluate the applicability of this method, 100 clinical samples were collected, of which 20 were from clinically diagnosed ALL patients, 60 were from non-acute lymphoblastic leukemia patients, and 20 were from normal healthy volunteers. Table 3 shows a specificity of 94% and a positive rate of 90%, while clinical sample specific information is shown in Table 2. Obviously, the ALL group is significantly different from the non-ALL group and the normal group as shown in Fig. 5. These results indicate that the fluorescence method can be applied for the detection of acute leukemia in blood samples of clinical patients.

4. Conclusion

In this work, we successfully developed a non-labeled signal sensitized fluorescence method for the detection of leukemia based on the characteristics of nucleic acid aptamer sensitized rare earth Tb^{3+} fluorescence. Compared with known cancer cell assay methods, this strategy has some superior features. First, the strategy of detection is inexpensive and convenient because no labels are required. Second, the affinity, stability, and specificity of the aptamer bound by Tb^{3+} are greatly enhanced under optimal conditions. Lastly, it is applicable for many types of cancer cells that use different aptamers to identify probes. Therefore, this simple, rapid, sensitive, universal and specific cancer cell detection strategy provides a new approach for the detection of cancer cells by the label-free fluorescence method. Compared with the antigen–antibody sandwich technique, this method shortens the detection time, enabling rapid analysis and formulation of treatment plans for patients as it provides a detailed classification of leukemia in real-time samples.

Conflicts of interest

There are no conflicts of interest to declare.

Acknowledgements

References

1 H. M. Meng, H. Liu, H. Kuai, R. Peng, L. Mo and X. B. Zhang, *Chem. Soc. Rev.*, 2016, **45**, 2583–2602.
2 J. Munoz, N. Shah, K. Rezvani, C. Hosing, C. M. Bollard, B. Oran, A. Olson, U. Popat, J. Molldrem, I. K. McNiece and E. J. Shpall, *Stem Cells Transl. Med.*, 2014, **3**, 1435–1443.
3 R. L. Siegel, S. A. Fedewa, K. D. Miller, A. Goding-Sauer, P. S. Pinheiro, D. Martinez-Tyson and A. Jemal, *CA-Cancer J. Clin.*, 2015, **65**, 457–480.
4 S. C. Chan, W. L. Yau, W. Wang, D. K. Smith, F. S. Sheu and H. M. Chen, *J. Pept. Sci.*, 1998, **4**, 413–425.
5 S. Boddington, T. D. Henning, E. J. Sutton and H. E. Daldrup-Link, *J. Visualized Exp.*, 2008, **13**, 685.
6 S. Choi, J. Yu, S. A. Patel, Y. L. Tzeng and R. M. Dickson, *Photochem. Photobiol. Sci.*, 2011, **10**, 109–115.
7 H. Shi, Z. Tang, Y. Kim, H. Nie, Y. F. Huang, X. He, K. Deng, K. Wang and W. Tan, *Chem. – Asian J.*, 2010, **5**, 2209–2213.
8 K. Pulford, N. Lecointe, K. Leroy-Viard, M. Jones, D. Mathieu-Mahul and D. Y. Mason, *Blood*, 1995, **85**, 675–684.
9 M. Doan, I. Vorobjev, P. Rees, A. Filby, O. Wolkenhauer, A. E. Goldfeld, J. Lieberman, N. Barteneva, A. E. Carpenter and H. Hennig, *Trends Biotechnol.*, 2018, **36**, 649–652.
10 G. Rymkiewicz, B. Grygalewicz, M. Chechlinska, K. Blachnio, Z. Bystydzienski, J. Romejko-Jarosinska, R. Woroniecka, M. Zajdel, K. Domanska-Czyz and D. Martin-Garcia, *Mod. Pathol.*, 2018, **31**, 732–743.
11 L. M. Neckers, W. K. Funkhouser, J. B. Trepel, J. Cossman and H. G. Gratzner, *Exp. Cell Res.*, 1985, **156**, 429–438.
12 I. B. Rozenvald, M. D. Richardson, L. Brock and R. L. Maiese, *Arch. Pathol. Lab. Med.*, 2017, **141**, 837–840.
13 E. A. Morgan, H. Yu, J. L. Pinkus and G. S. Pinkus, *Am. J. Clin. Pathol.*, 2013, **139**, 220–230.
14 L. C. Ho, W. C. Wu, C. Y. Chang, H. H. Hsieh, C. H. Lee and H. T. Chang, *Anal. Chem.*, 2015, **87**, 4925–4932.
15 L. Yan, H. Shi, X. He, K. Wang, J. Tang, M. Chen, X. Ye, F. Xu and Y. Lei, *Anal. Chem.*, 2014, **86**, 9271–9277.
16 D. Shangguan, L. Meng, Z. C. Cao, Z. Xiao, X. Fang, Y. Li, D. Cardona, R. P. Witek, C. Liu and W. Tan, *Anal. Chem.*, 2008, **80**, 721–728.
17 M. Ye, J. Hu, M. Peng, J. Liu, J. Liu, H. Liu, X. Zhao and W. Tan, *Int. J. Mol. Sci.*, 2012, **13**, 3341–3353.
18 A. Ganji, A. Varasteh and M. Sankian, *J. Drug Targeting*, 2016, **24**, 1–12.
19 Q. Shen, C. Peng, Y. Zhan, L. Fan, M. Wang, Q. Zhou, J. Liu, X. Lv, Q. Tang, J. Li, X. Huang and J. Xia, *Int. J. Nanomed.*, 2016, **11**, 2133–2146.
20 B. Mondal, S. Ramlal, P. S. Lavu, B. N and J. Kingston, *Front. Microbiol.*, 2018, **9**, 179.
21 M. Mascini, I. Palchetti and S. Tombelli, *Angew. Chem., Int. Ed.*, 2012, **51**, 1316–1332.
22 S. Philippou, N. P. Mastroyiannopoulos, N. Makrides, C. W. Lederer, M. Kleanthous and L. A. Phylactou, *Mol. Ther.–Nucleic Acids*, 2018, **10**, 199–214.

23 X. Li, Y. Peng, Y. Chai, R. Yuan and Y. Xiang, *Chem. Commun.*, 2016, **52**, 3673–3676.

24 Y. Tan, X. Wei, Y. Zhang, P. Wang, B. Qiu, L. Guo, Z. Lin and H. H. Yang, *Anal. Chem.*, 2015, **87**, 11826–11831.

25 J. Ni, W. Yang, Q. Wang, F. Luo, L. Guo, B. Qiu, Z. Lin and H. Yang, *Biosens. Bioelectron.*, 2018, **105**, 182–187.

26 Y. Wang, Z. Li, H. Li, M. Vuki, D. Xu and H. Y. Chen, *Biosens. Bioelectron.*, 2012, **32**, 76–81.

27 H. Li, M. Wang, C. Wang, W. Li, W. Qiang and D. Xu, *Anal. Chem.*, 2013, **85**, 4492–4499.

28 S. Feng, C. Chen, W. Wang and L. Que, *Biosens. Bioelectron.*, 2018, **105**, 36–41.

29 C. Chen, Z. Yang and X. Tang, *Med. Res.*, 2018, **38**, 829–869.

30 Y. Yao, X. Wang, W. Duan and F. Li, *Analyst*, 2018, **143**, 709.

31 P. Mallikaratchy, Z. Tang, S. Kwame, L. Meng, D. Shangguan and W. Tan, *Mol. Cell. Proteomics*, 2007, **6**, 2230–2238.

32 Y. X. Zou, S. Huang, Y. Liao, X. Zhu, Y. Chen, L. Chen, F. Liu, X. Hu, H. Tu and L. Zhang, *Chem. Sci.*, 2018, **9**, 2842–2849.

33 D. Shangguan, Y. Li, Z. Tang, Z. C. Cao, H. W. Chen, P. Mallikaratchy, K. Sefah, C. J. Yang and W. Tan, *Proc. Natl. Acad. Sci. U. S. A.*, 2006, **103**, 11838–11843.

34 S. M. Taghdisi, K. Abnous, F. Mosaffa and J. Behravan, *J. Drug Targeting*, 2010, **18**, 277–281.

35 N. M. Danesh, P. Lavaee, M. Ramezani, K. Abnous and S. M. Taghdisi, *Int. J. Pharm.*, 2015, **489**, 311–317.

36 A. Fang, H. Chen, H. Li, M. Liu, Y. Zhang and S. Yao, *Biosens. Bioelectron.*, 2017, **87**, 545–551.

37 J. Yuan and G. Wang, *J. Fluoresc.*, 2005, **15**, 559–568.

38 Z. Ye, J. Chen, G. Wang and J. Yuan, *Anal. Chem.*, 2011, **83**, 4163–4169.

39 K. L. Fu and C. Turro, *J. Am. Chem. Soc.*, 2009, **121**, 1–7.

40 M. K. Johansson, R. M. Cook, J. Xu and K. N. Raymond, *J. Am. Chem. Soc.*, 2004, **126**, 16451–16455.

41 W. Yueteng, L. Ru, W. Yaling, Z. Yuliang, C. Zhifang and G. Xueyun, *Analyst*, 2013, **138**, 2302–2307.

42 H. Shi, D. Li, F. Xu, X. He, K. Wang, X. Ye, J. Tang and C. He, *Analyst*, 2014, **139**, 4181–4184.

43 Y. Pan, M. Guo, Z. Nie, Y. Huang, C. Pan, K. Zeng, Y. Zhang and S. Yao, *Biosens. Bioelectron.*, 2010, **25**, 1609–1614.

44 J. Zhu, T. Nguyen, R. Pei, M. Stojanovic and Q. Lin, *Lab Chip*, 2012, **12**, 3504–3513.

45 J. Yin, X. He, K. Wang, F. Xu, J. Shangguan, D. He and H. Shi, *Anal. Chem.*, 2013, **85**, 12011–12019.